Femtosecond-laser-induced creation of G and W color centers in silicon-on-insulator substrates

Hugo Quard[1,*] Mario Khoury,[2] Andong Wang[3] Tobias Herzig[4] Jan Meijer,[4]
Sébastien Pezzagna,[4] Sébastien Cueff[1] David Grojo[3] Marco Abbarchi[2,5,†] Hai Son Nguyen[1,6]
Nicolas Chauvin[1] and Thomas Wood[1]

[1]*Ecole Centrale de Lyon, INSA Lyon, Université Claude Bernard Lyon 1, CPE Lyon, CNRS, INL, UMR5270, Ecully 69130, France*

[2]*Aix-Marseille Université, CNRS, Université de Toulon, IM2NP, UMR 7334, Marseille F-13397, France*

[3]*Aix-Marseille University, CNRS, LP3, UMR7341, Marseille 13009, France*

[4]*Division of Applied Quantum Systems, Felix-Bloch Institute for Solid-State Physics, Universität Leipzig, Linnéestrasse 5, Leipzig 04103, Germany*

[5]*Solnil, 95 Rue de la République, Marseille 13002, France*

[6]*Institut Universitaire de France (IUF), F-75231 Paris, France*

The creation of fluorescent defects in silicon is a key stepping stone toward assuring the integration perspectives of quantum photonic devices into existing technologies. Here, we demonstrate the creation, by femtosecond laser annealing, of W and G centers in commercial silicon on insulator (SOI) previously implanted with $^{12}C^+$ ions. Their quality is comparable to that found for the same emitters obtained with conventional implantation processes; as quantified by the photoluminescence radiative lifetime, the broadening of their zero-phonon line (ZPL), and the evolution of these quantities with temperature. In addition to this, we show that both defects can be created without carbon implantation and that we can erase the G centers by annealing while enhancing the W-center emission. These demonstrations are relevant to the deterministic and *operando* generation of quantum emitters in silicon.

I. INTRODUCTION

Point defects in silicon have been intensively studied over the past few years for the creation of silicon-based quantum devices [1]. Quantum light sources are key devices that are potentially exploitable for quantum computing or quantum networks or for the implementation of quantum cryptography protocols. Thanks to the device-friendly environment, single-photon sources and spin-photon interfaces could be readily integrated within existing electronic and photonic platforms.

Among all the different optically active defects in silicon [2–10], two that are often studied are W [11–16] and G centers [1,17–35]. W centers are composed of three interstitial Si atoms and recent theoretical works have revealed that these defects probably have a I_3-V configuration [36]. The optically active form of a G center is made of two C atoms in substitutional sites linked to an interstitial Si atom [17], as represented in Fig. 1(a).

Numerous procedures can be used to fabricate W or G centers, such as silicon [12] or carbon implantation followed by proton irradiation [19,22], electron irradiation [3], focused-ion-beam (FIB) implantation [8], pulsed ion beams [37], and reactive ion etching [38,39]. All these methods involve the use of ion implanters or accelerators. They are relatively bulky and expensive approaches that require several steps (e.g., for G centers, carbon implantation, annealing, and proton implantation) in order to create a light emitter. Furthermore, the most advanced methods using focused ion beams [8] are intrinsically stochastic and the number of quantum emitters per ion impact is not precisely controlled.

A further method, that can be used to create point defects, is laser annealing—also called laser doping. The use of a laser has been shown to be a viable approach for integrating quantum emitters in Si grown by the float-zone method [40], in δ-doped Si [41], or in p-doped Si [42]. Both W and G centers can be obtained in p-doped Si [16] as well as in n-type Si implanted with $^{29}Si^+$ ions [2]. However, the creation of these defects has usually been unintentional, induced with laser pulses longer than 4 ns and in bulk Si substrate.

---

*Corresponding author: hugo.quard@insa-lyon.fr

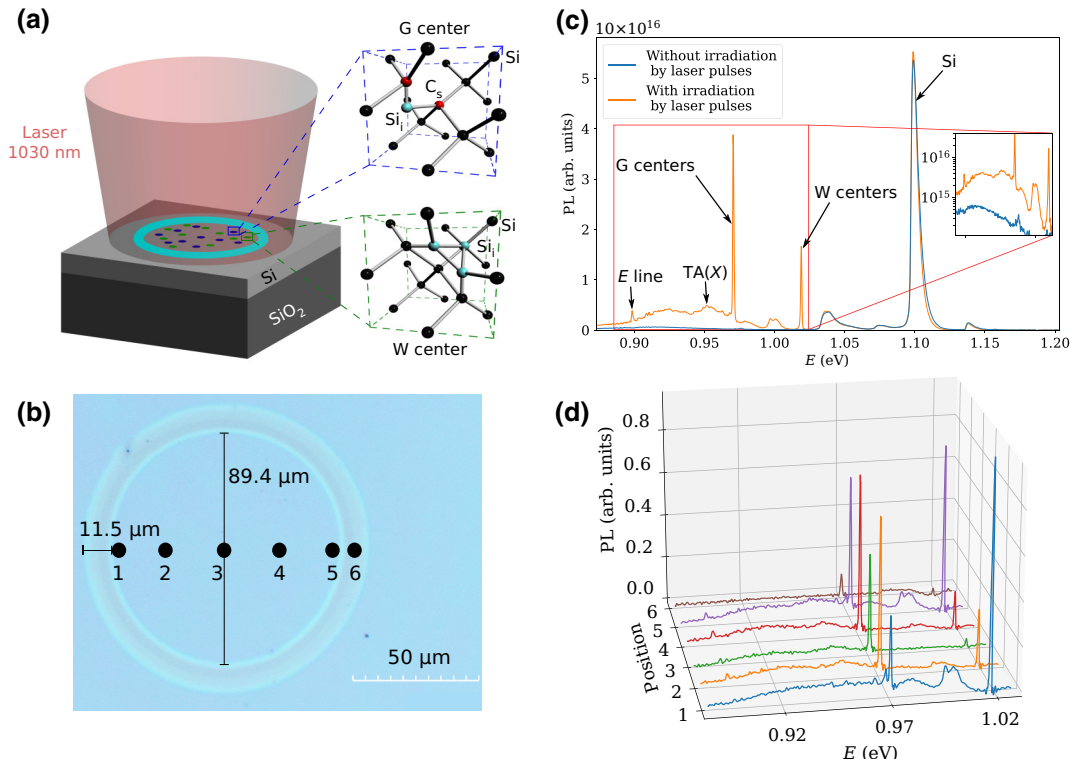†Corresponding author: marco.abbarchi@im2np.fr

FIG. 1. (a) A schematic representation of the laser-irradiation process used to create G and W centers. (b) An optical-microscope image of an area irradiated with three pulses, having an energy of 218 µJ. (c) A comparison of the macro-PL spectra at 12 K of an area not irradiated by laser pulses and an area irradiated by three pulses. (d) A comparison of the micro-PL spectra at 11 K of the different positions noted on the optical microscope image and corrected by the background spectra obtained with nonannealed SOI (for the correction applied, see the Supplemental Material [43]).

In this paper, we address the creation of W and G centers by femtosecond laser annealing, with the process being investigated for the first time on SOI substrates, taking both C-doped and pristine SOI wafers as starting points. The quality of these defects is confirmed by continuous-wave (cw) and time-resolved photoluminescence (PL) measurements. The temperature dependence of the emitters, their broadening, and their lifetimes are comparable to those reported with standard fabrication methods, accounting for the high quality of our approach based on femtosecond laser pulses. We also demonstrate that the carbon implantation step is not necessary to create the light emitters. Finally, by low-temperature annealing, we can selectively erase the G centers while improving the brightness of the W-center emission.

II. SAMPLE DESCRIPTION AND EXPERIMENTAL SETUP

The samples are SOI wafers featuring a 220-nm top silicon layer and a 2-µm buried oxide layer, some of which has been implanted with $^{12}C^+$ ions. The beam energy was set to 34 keV in order to implant the carbon ions halfway into the top silicon layer and two different fluences were explored, namely, 1×10^{12} and 1×10^{13} ions/cm^2.

The implantation was followed by a flash annealing under an N$_2$ atmosphere for 20 s at 1000 °C, to remove lattice damage [19].

The samples were then irradiated by laser pulses focused with a 750-mm planoconvex lens under ambient conditions, differing from location to location by the number of pulses used (from one to five) and by the energy of the pulses (95, 143, 175, and 218 µJ), to supply the energy necessary to reorganize the crystal lattice and create emitting defects in silicon. This step is schematically represented in Fig. 1(a). The Gaussian laser beam used was centered at 1030 nm, with pulses of a duration of less than 200 fs. The waist of the beam was $w_0 = 178$ µm and the repetition frequency of the pulses was 1 kHz. The samples were created in pairs, sharing the same carbon-implantation parameters, of which only one of the two underwent a second annealing under an N$_2$ atmosphere for 5 min at 125 °C after the laser annealing.

The PL measurements were performed at low temperature, the samples being cooled down with a closed-cycle helium-cooled cryostat. For the macro-PL measurements, optical pumping was performed with a cw laser diode at 405 nm, focused onto the sample with a spot diameter of approximately 75 µm. A Cassegrain objective was used to collect the PL emission, with a numerical aperture between

0.15 and 0.4. For the micro-PL measurements, the optical pumping was performed with a 780-nm diode-pumped solid-state laser. The signal was detected in a confocal configuration with a microscope objective (NA = 0.4), allowing a spot diameter of approximately 10 μm for the pump. In both cases, the collected signal was dispersed by a spectrometer and detected by a liquid-nitrogen-cooled InGaAs detector, enabling spectral detection from 900 to 1600 nm. For the time-resolved PL, a 515-nm laser emitting 200-fs pulses and a 54-MHz repetition rate was used for the optical pumping and the detection was performed with an InGaAs photodiode.

III. RESULTS

A. Creation of G and W centers

For the highest pulse energy investigated (218 μJ), the laser pulses created a ring visible under an optical microscope at the surface of the irradiated parts of the sample, around the point of impact of the laser beam, as shown in Fig. 1(b). The creation of this circle is specific to the ultrafast quenching conditions accessible with femtosecond laser irradiation. It results from the melting of the top layer of Si, which resolidifies in different states due to the temperature gradient, which in turn causes spatial variation in the solidification kinetics. The ring corresponds to amorphous Si, whereas the central part is constituted of recrystallized Si [42,44]. The outer contour of the ring, shown in Fig. 1(a), corresponds to a local fluence of about 330 mJ/cm^2 that matches well with the measured threshold for Si surface amorphization in a previous work using the same laser [45].

The PL signal from these areas reveals the creation of both G and W centers, as shown by the orange curve in Fig. 1(c), exhibiting the zero-phonon lines (ZPLs) of the two emitters, at 1.019 eV for W centers and 0.97 eV for G centers, as well as their typical phonon sidebands [3,22,36].

On the same sample, we also collected the PL emission in areas that were not targeted by the laser [blue curve in the Fig. 1(c)]. The corresponding spectrum exhibits only the typical Si signal at 1.1 eV, accompanied with the relative phonon sidebands.

For lower laser fluences, the ring is not observed (see the Supplemental Material [43]) and there is a lack of PL emission from the W and G centers, suggesting the crucial role of the melting and recrystallization steps in rearranging the atoms to form the emitters.

We also studied the influence of the number of pulses on the intensity, the position, and the width of the ZPLs (see the Supplemental Material [43]). No trend can be seen from one sample to another, which suggests that at each pulse there is melting of the silicon and therefore the destruction of preexisting defects. New defects are then created during recrystallization.

B. Spatial distribution of G and W centers

To investigate the distribution of centers within the recrystallized region, micro-PL measurements were conducted. The spectra, adjusted for background PL originating from the SOI wafer itself, are presented in Fig. 1(d). The original micro-PL spectra and details regarding the correction procedure are provided in the Supplemental Material [43]. Figure 1(d) unveils notable differences in the distribution of the G and W centers. Notably, the signal of the W centers appears brighter near the amorphous ring [positions 1 and 5 in Figs. 1(b) and 1(d)] compared to the center of the recrystallized area (position 3). It is known that there is a strong dependence between the concentration of self-interstitial clusters and the cooling rate during the Si recrystallization [16]. Therefore, it is not surprising to observe a strong modification of the W-center emission intensity from the center to the border of the recrystallized area. In contrast, G centers exhibit a more random distribution within the recrystallized area, reflecting the random distribution of carbon throughout the sample. The Supplemental Material [43] includes a graph depicting the maxima of the ZPLs of both centers with regard to their position.

Micro-PL measurements on the amorphous ring [position 6 in Fig. 1(b)] reveal significantly weaker signals for G and W centers compared to the signals obtained in the recrystallized area [Fig. 1(d)]. We attribute these signals to defects located in proximity to the edge of the amorphous ring.

C. Influence of the carbon fluence

In this section, we focus on the influence of the fluence of implanted carbon on the PL of the centers. In Fig. 2(a), we present the macro-PL spectra of three samples that differ by virtue of the carbon fluence used during the implantation. For each spectrum, the Si signal is of the same order of magnitude, which allows a direct comparison between the spectra.

The ZPL intensity of the G centers increases when increasing the carbon fluence, which is consistent with previous findings [19] for emitters created after proton irradiation.

For pristine samples (i.e., no carbon implantation), the signals of the G and W centers appear with an amplitude that is about an order of magnitude lower with respect to their implanted counterparts. We interpret the creation of G centers in carbon-free samples as an effect of incorporation of residual C present in small quantities in the native oxide (e.g., unintentionally deposited after the manufacturing process of the SOI wafer). We have verified that by oxidation of the Si in a rapid thermal process before the laser annealing, the signal from G centers disappears, confirming that the C contamination comes from impurities in the native oxide and that can be efficiently
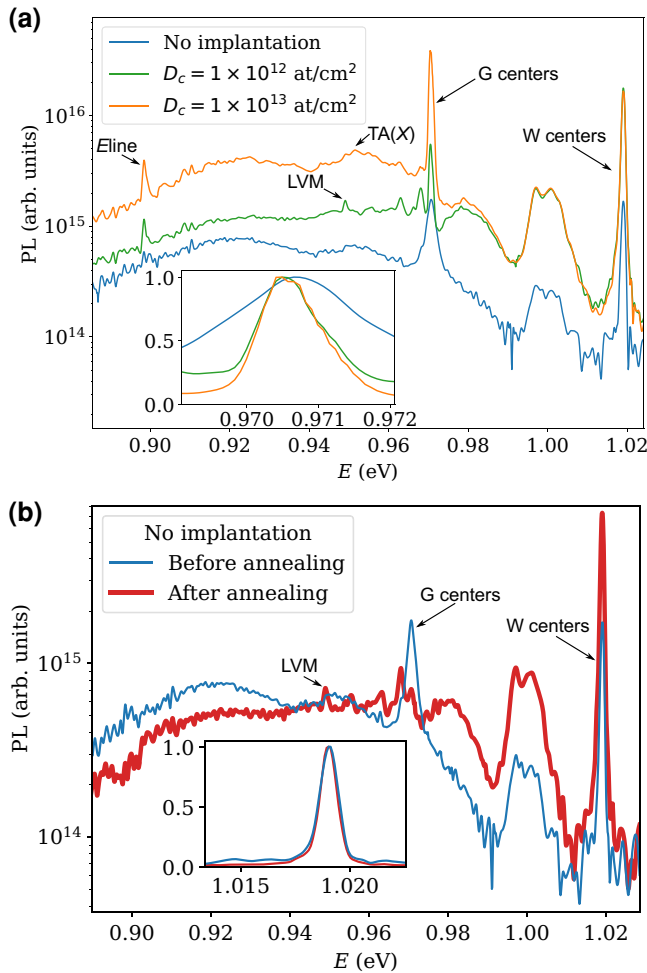
FIG. 2. All the spectra were measured at 12 K, with excitation by a laser diode at 405 nm. (a) The macro-PL spectra obtained for samples irradiated by three laser pulses with an energy of 218 μJ. Each sample is differentiated by the fluence of implanted carbon, D_C. The inset represents the normalized ZPL of the G centers. (b) A comparison between the macro-PL spectra obtained for two samples irradiated by three laser pulses with an energy of 218 μJ. The two samples have not undergone carbon implantation and one of them has undergone a second annealing under an N_2 atmosphere for 5 min at 125 °C. The inset represents the normalized ZPL of the W centers.

passivated by thermal oxidation (see the Supplemental Material [43]).

As for the W centers, this result shows that the implantation step disrupts the crystalline organization and creates more interstitial Si. However, even if defects are created in smaller numbers in the pristine sample, they have the same optical properties as those obtained with the implantation step, namely, a ZPL with the same full width at half maximum (FWHM) (see the Supplemental Material [43]), since the creation process of the W centers is the same in both cases. In contrast, for G centers, the creation process differs due to the origin of the C, resulting in a broadening and a

slight blue shift of the ZPL of the nonimplanted sample, as depicted in Fig. 2(a).

D. Effect of a 5-min annealing at 125 °C

We now investigate the effect of a 5-min annealing at 125 °C on the PL signal of these laser-created emitting centers. After annealing, nonimplanted samples display only W-center emission that is enhanced by a factor of 4 with respect to nonannealed samples, whereas that of the G centers disappears [Fig. 2(b)]. Moreover, the FWHM of the ZPL of the W centers is not modified by the treatment, as shown in the inset of Fig. 2(b). The increase in the W-center PL emission has been reported by several groups after annealing in the 100–200 °C range [46–49]. This is explained by the annealing-induced breaking of Si self-interstitial (Si_i) clusters, leading to the migration of these Si_i, which are potentially captured by remaining clusters. Consequently, the annealing alters the cluster size distribution, resulting in an increased number of three Si_i clusters (W centers). Moreover, the migration of Si_i could account for the disappearance of the G-center emission. According to Davies and Kun [50], Si_i may be captured by G centers, forming new complexes.

The annihilation of the G centers after an annealing is also observed for carbon-implanted samples and the resulting spectrum is comparable to that obtained for pristine samples when normalized by the maximum of the ZPL of the W centers. Therefore, we demonstrate that we can create and isolate W centers without any implantation step, with optical properties comparable to those obtained with implantation.

E. Recombination dynamics of G centers

We have performed time-resolved PL measurements on the brighter sample, namely, the sample with the highest fluence of C implanted, filtering the PL signal with a short-pass filter at 0.99 eV to eliminate the major contribution of the W centers (Fig. 3). The PL decay is well fitted by a monoexponential function (plus a constant), providing a characteristic lifetime of 5.9 ns, which is consistent with conventional G centers obtained by coimplantation of carbon and proton irradiation, for which the lifetime is about 5–6 ns [22,33]. Therefore, G centers created with both protocols have the same excited-state lifetime. As the radiative yield of the G centers is less than 10% at 30 K [33], the measured decay rate is strongly related to nonradiative channels even at cryogenic temperatures.

The constant used to adjust the fit is ascribed to the contribution of a longer decay time corresponding to the phonon sideband of the W centers: these defects have lifetimes ranging from 3 to 30 ns [36]. Owing to our excitation pulses being repeated every 18 ns, an overlap of the PL decays coming from the phonon sideband of the W centers can contribute to the time-resolved spectra. We therefore cannot measure the lifetime of the W centers.
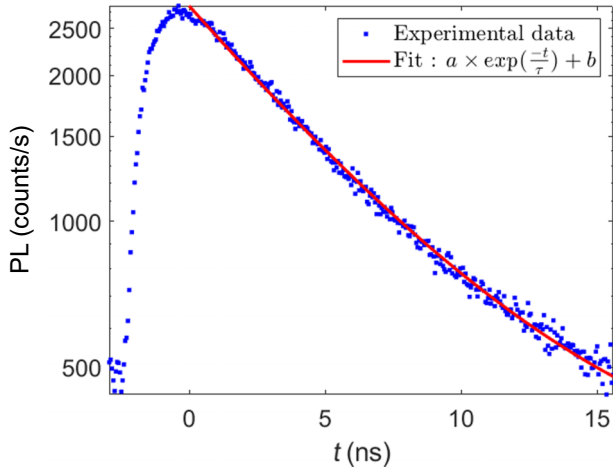
FIG. 3.   The time-resolved PL signal obtained at 12 K with a pulsed laser at 515 nm with a short-pass filter in energy (0.99 eV) to eliminate the contribution of the ZPL of the W centers and a large part of their phonon sideband. The experimental data (blue points) are fitted by a monoexponential function adjusted by a constant b (red curve).

F. Temperature dependence of the ZPL

The ZPL energy as a function of temperature is represented in Fig. 4(b). The experimental data are fitted with an expression proposed by Pässler [51]:

$$\Delta E(T) = E_{ZPL}(T) - E_0$$

$$= -\frac{\alpha\Theta_p}{2}\left[\sqrt[p]{1+\left(\frac{2T}{\Theta_p}\right)^p}-1\right], \quad (1)$$

where E_0 (meV) is the limit of the ZPL energy when $T \to 0$ K, α (meV/K) is the slope of the curve—namely, the entropy—for $T \to \infty$, Θ_p (K) is the average temperature of the phonons, and p is a dimensionless parameter.

The thermal red shift for W centers evolves proportionally to T^4 [52], whereas for G centers it evolves proportionally to T^3, consistent with previous observations [22]. These fits provide the average temperature of the phonons coupled with the defects. If we convert the obtained values to energies, we find $E_{phW} = 7 \pm 1$ meV for W centers and $E_{phG} = 16 \pm 2$ meV for G centers. For the latter, the energy obtained is close to that of transverse acoustic (TA) phonons at the X point of the Brillouin zone [9], namely, 20 meV. Therefore, we conclude that the defect has coupled preferentially with TA(X) phonons. As for W centers, the obtained value does not correspond to a typical phonon energy in silicon and it is lower than the TA(X) energy. A possible explanation for this observation will be given in the following paragraphs.

In Fig. 4(c), we present the FWHM of the ZPLs as a function of temperature. The experimental data are well fitted by the following model that describes the broadening of a ZPL with heating [53]:

$$\Gamma = \Gamma_0 + a\left[\exp\left(\frac{-\Omega}{k_B T}\right) - 1\right]^{-1}, \quad (2)$$

where Γ_0 is the zero-temperature limit of the FWHM, the second term accounts for the coupling between the phonons and the emitters, a represents the intensity, and Ω is the typical energy of this coupling.
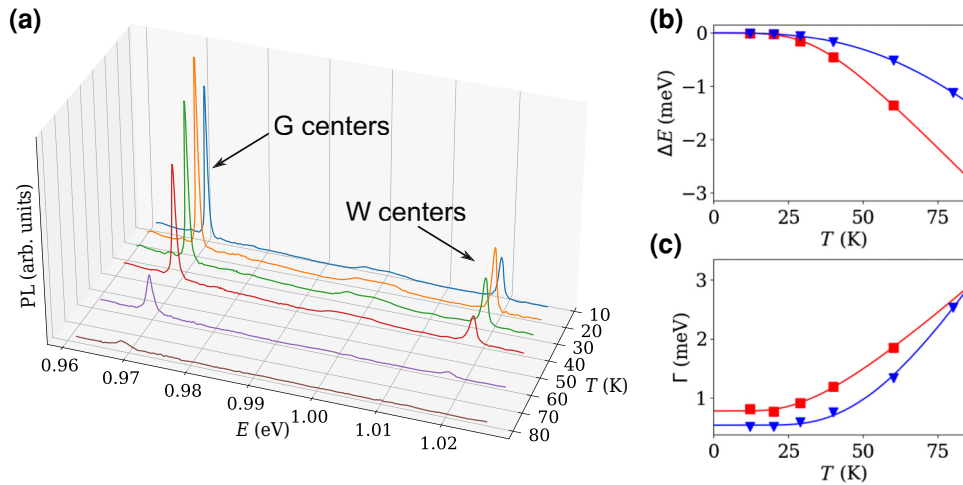

FIG. 4.   (a) Temperature-dependant macro-PL spectra centered around the ZPLs of the G and W centers in the temperature range from 12 K to 80 K. (b) Variation of the energies at the center of the ZPLs of the G centers (blue triangles) and W centers (red squares) as a function of temperature. The symbols represent the experimental data and the lines the fits given by Eq. (1). The fitting parameters are $E_{0W} = 1018.69 \pm 0.02$ meV, $\alpha_W = 0.06 \pm 0.01$ meV/K, $\Theta_W = 76 \pm 15$ K, and $P_W = 4.2 \pm 1.1$ for the W centers and $E_{0G} = 970.194 \pm 0.003$ meV, $\alpha_G = 0.07 \pm 0.01$ meV/K, $\Theta_G = 186 \pm 29$ K, and $P_W = 3.0 \pm 0.1$ for the G centers. (c) The evolution of the FWHM of the ZPLs of the G centers (blue triangles) and W centers (red squares) as a function of temperature. The symbols represent the experimental data and the lines the fits given by Eq. (2). The fitting parameters are $\Gamma_{0W} = 0.78 \pm 0.03$ meV, $a_W = 5 \pm 1$ meV, and $\Omega_W = 9 \pm 1$ meV for the W centers and $\Gamma_{0G} = 0.54 \pm 0.03$ meV, $a_W = 20 \pm 5$ meV, and $\Omega_W = 17 \pm 1$ meV for the G centers.

The zero-temperature limit obtained for G centers with our procedure, namely, $\Gamma_{0G} = 0.54 \pm 0.03$ meV, is of the same order of magnitude as that obtained for an ensemble of G centers created by proton irradiation (0.3 ± 0.03 meV) [22]. The slightly larger value obtained in our case can be explained by the simultaneous presence of G centers and Si self-interstitials, which could slightly broaden the signal obtained for the ensemble of defects.

For ensembles of W centers, to date, no study has been conducted for ZPL broadening. The study of individual W centers [32] has shown a zero-temperature limit below 0.1 meV. However, the energy differences between the ZPLs from one defect to another are within 1 meV owing to local variations in the emitter environment. Therefore, the value of $\Gamma_{0G} = 0.78 \pm 0.03$ meV that we have obtained is consistent with single-defect investigation when taking into account the dispersion in energy of the ZPLs.

For G and W centers, the typical energies E_{ph} and Ω that we have obtained with the fits of the broadening and the red shift of ZPLs overlap, taking uncertainties into account. This allows us to give a probable explanation for the low value obtained for E_{phW}. Indeed, the typical energy obtained with the fit of the broadening (Ω_W) could also be interpreted as the activation energy of the excitonic transition to the first excitonic state from the ground state [54], which could explain why we obtain a value lower than the typical energy of phonons in Si.

IV. DISCUSSION

The relevance of our work lies in the possibility of deterministically creating at least one quantum emitter in Si: in analogy with SiC and diamonds, femtosecond laser pulses can, in principle, be used to form the emitters *in situ* and *operando*, while monitoring the emission from newly formed defects on a pulse-by-pulse basis [55,56]. This method also allows us to reduce the area of creation of the emitters down to the size of the laser spot, as shown in Fig. 1, which demonstrates that the emitting centers are created only in the irradiated areas. Even if we do not reach the precision of FIB, this method is cheaper and easier to implement, which is promising for the large-scale creation of emitters. Moreover, we have demonstrated that W and G centers created in C-implanted Si have optical properties and recombination dynamics that are adequate when compared with the literature, which proves that we have obtained emitters with the same quality as those obtained by other fabrication methods.

We have also demonstrated that the implantation step is not necessary to create W and G centers, as we have collected the PL signatures of both centers from pristine samples. Such samples contain only residual carbon incorporated in the surface native oxide on the SOI after the manufacturing of the wafer, which implies a low concentration of carbon. This leads to the creation of low-density G centers, which is confirmed not only by the low intensity of the ZPL of the G centers but also by its broadening and blue shift compared to the implanted samples (see the inset of Fig. 2). Indeed, Zhiyenbayev *et al.* have demonstrated that the increase of internal strain due to a high fluence of implanted carbons leads to a red shift of the ZPL of the G centers and reduces their inhomogeneous broadening [35]. As for W centers, they have the same optical properties in implanted and nonimplanted samples. We have demonstrated a way to annihilate G centers while slightly enhancing the PL of the W centers by carrying out an annealing at 125 °C during 5 min. This phenomenon is opposite to what was expected, since it has been demonstrated that the intensity of the ZPL of the G centers created with carbon implantation followed by proton irradiation can be increased by a factor of 8 with such thermal treatment [21]. It is worth noting that in the sample of Berhanuddin *et al.*, only G centers were created, whereas in our case we have both W and G centers, which could explain the difference in behavior of the G centers.

V. CONCLUSIONS

In this paper, we have demonstrated the creation of G and W centers simultaneously in carbon-implanted SOI by femtosecond laser annealing. The quality of these defects is comparable to those obtained by the usual well-established methods in the literature. We have also demonstrated that we can create G and W centers without any implantation step. However, G centers created with this method have a ZPL broader than those obtained with carbon implantation. Furthermore, we have demonstrated that an annealing at low temperature annihilates G centers while slightly enhancing the PL emission of the W centers. Therefore, we have proved that we can create and purify W centers of good quality without any implantation steps, which allows us to create W centers at low cost, on demand, and in a restricted area, of a size close to the cross section of the laser spot. This represents a step forward for the deterministic creation of W centers in photonic structures. Indeed, with this method it is possible to precisely position the defects in the structures and it is also conceivable to have control over the density of defects created by studying, in more detail, the influence of the number of pulses and their energy. This last aspect could even lead to the study of single emitters, assuming that we manage to create the W centers in sufficiently low density.

Note added.—We recently became aware of a paper by Jhuria *et al.*, wherein they have demonstrated the creation of both centers using femtosecond laser pulses. However, they have employed significantly different experimental parameters, including shorter pulses, a different wavelength, and a *p*-type SOI substrate [57].

[1] M. Khoury and M. Abbarchi, A bright future for silicon in quantum technologies, J. Appl. Phys. **131,** 200901 (2022).

[2] M. S. Skolnick, A. G. Cullis, and H. Webber, Defect photoluminescence from pulsed-laser-annealed ion-implanted Si, Appl. Phys. Lett. **38,** 464 (1981).

[3] K. Thonke, H. Klemisch, J. Weber, and R. Sauer, New model of the irradiation-induced 0.97-eV (G) line in silicon: A Cs-Si* complex, Phys. Rev. B **24,** 5874 (1981).

[4] A. N. Safonov, E. C. Lightowlers, G. Davies, P. Leary, R. Jones, and S. Öberg, Interstitial-carbon hydrogen interaction in silicon, Phys. Rev. Lett. **77,** 4812 (1996).

[5] L. Bergeron, C. Chartrand, A. T. K. Kurkjian, K. J. Morse, H. Riemann, N. V. Abrosimov, P. Becker, H.-J. Pohl, M. L. W. Thewalt, and S. Simmons, Silicon-integrated telecommunications photon-spin interface, PRX Quantum **1,** 020301 (2020).

[6] A. Durand, Y. Baron, W. Redjem, T. Herzig, A. Benali, S. Pezzagna, J. Meijer, A. Y. Kuznetsov, J.-M. Gérard, I. Robert-Philip, et al., Broad diversity of near-infrared single-photon emitters in silicon, Phys. Rev. Lett. **126,** 083602 (2021).

[7] W. Redjem, A. J. Amsellem, F. I. Allen, G. Benndorf, J. Bin, S. Bulanov, E. Esarey, L. C. Feldman, J. F. Fernandez, J. G. Lopez, et al., Defect engineering of silicon with ion pulses from laser acceleration, arXiv:2203.13781.

[8] M. Hollenbach, N. Klingner, N. S. Jagtap, L. Bischoff, C. Fowley, U. Kentsch, G. Hlawacek, A. Erbe, N. V. Abrosimov, M. Helm, et al., Wafer-scale nanofabrication of telecom single-photon emitters in silicon, Nat. Commun. **13,** 7683 (2022).

[9] V. Ivanov, J. Simoni, Y. Lee, W. Liu, K. Jhuria, W. Redjem, Y. Zhiyenbayev, C. Papapanos, W. Qarony, B. Kante, et al., Effect of localization on photoluminescence and zero-field splitting of silicon color centers, Phys. Rev. B **106,** 134107 (2022).

[10] W. Redjem, A. Durand, T. Herzig, A. Benali, S. Pezzagna, J. Meijer, A. Y. Kuznetsov, H. S. Nguyen, S. Cueff, J.-M. Gérard, et al., Single artificial atoms in silicon emitting at telecom wavelengths, Nat. Electron. **3,** 738 (2020).

[11] G. Davies, E. C. Lightowlers, and Z. E. Ciechanowska, The 1018 meV (W or I$_1$) vibronic band in silicon, J. Phys. C **20,** 191 (1987).

[12] S. Buckley, J. Chiles, A. N. McCaughan, G. Moody, K. L. Silverman, M. J. Stevens, R. P. Mirin, S. W. Nam, and J. M. Shainline, All-silicon light-emitting diodes waveguide-integrated with superconducting single-photon detectors, Appl. Phys. Lett. **111,** 141101 (2017).

[13] G. Davies, E. C. Lightowlers, and Z. E. Ciechanowska, The 1018 meV (W or I$_1$) vibronic band in silicon, J. Phys. C **20,** 191 (1987).

[14] A. Carvalho, R. Jones, J. Coutinho, and P. R. Briddon, Density-functional study of small interstitial clusters in Si: Comparison with experiments, Phys. Rev. B **72,** 155208 (2005).

[15] S. M. Buckley, A. N. Tait, G. Moody, B. Primavera, S. Olson, J. Herman, K. L. Silverman, S. P. Rao, S. W. Nam, R. P. Mirin, et al., Optimization of photoluminescence from W centers in silicon-on-insulator, Opt. Express **28,** 16057 (2020).

[16] T. Menold, M. Ametowobla, and J. H. Werner, Signatures of self-interstitials in laser-melted and regrown silicon, AIP Adv. **11,** 055212 (2021).

[17] L. W. Song, X. D. Zhan, B. W. Benson, and G. D. Watkins, Bistable interstitial-carbon–substitutional-carbon pair in silicon, Phys. Rev. B **42,** 5765 (1990).

[18] K. Murata, Y. Yasutake, K.-i. Nittoh, S. Fukatsu, and K. Miki, High-density G-centers, light-emitting point defects in silicon crystal, AIP Adv. **1,** 032125 (2011).

[19] D. D. Berhanuddin, M. A. Lourenço, R. M. Gwilliam, and K. P. Homewood, Co-implantation of carbon and protons: An integrated silicon device technology compatible method to generate the lasing G-center, Adv. Func. Mater. **22,** 2709 (2012).

[20] H. Wang, A. Chroneos, C. A. Londos, E. N. Sgourou, and U. Schwingenschlögl, G-centers in irradiated silicon revisited: A screened hybrid density functional theory approach, J. Appl. Phys. **115,** 183509 (2014).

[21] D. D. Berhanuddin, Ph.D. thesis, Faculty of Engineering and Physical Sciences Advanced Technology Institute University of Surrey, Guildford, Surrey, 2015, available online at http://adsabs.harvard.edu/abs/2015PhDT.......332B.

[22] C. Beaufils, W. Redjem, E. Rousseau, V. Jacques, A. Y. Kuznetsov, C. Raynaud, C. Voisin, A. Benali, T. Herzig, S. Pezzagna, et al., Optical properties of an ensemble of G-centers in silicon, Phys. Rev. B **97,** 035303 (2018).

[23] D. Timerkaeva, C. Attaccalite, G. Brenet, D. Caliste, and P. Pochet, Structural, electronic, and optical properties of the C-C complex in bulk silicon from first principles, J. Appl. Phys. **123,** 161421 (2018).

[24] C. Beaufils, Ph.D. thesis, École doctorale : Information, Structures, Systèmes, Université Montpellier, 2019, available online at http://www.theses.fr/2019MONTS007.

[25] W. Redjem, Ph.D. thesis, École doctorale : Information, Structures, Systèmes, Université Montpellier, 2019, available online at https://tel.archives-ouvertes.fr/tel-0249 1663.

[26] L. Zhu, S. Yuan, C. Zeng, and J. Xia, Manipulating photoluminescence of carbon G-center in silicon metasurface with optical bound states in the continuum, Adv. Opt. Mat. **8,** 1901830 (2020).

[27] M. Hollenbach, Y. Berencén, U. Kentsch, M. Helm, and G. V. Astakhov, Engineering telecom single-photon emitters

in silicon for scalable quantum photonics, Opt. Express **28,** 26111 (2020).

[28] P. Udvarhelyi, B. Somogyi, G. Thiering, and A. Gali, Identification of a telecom wavelength single photon emitter in silicon, Phys. Rev. Lett. **127,** 196402 (2021).

[29] M. Hollenbach, N. S. Jagtap, C. Fowley, J. Baratech, V. Guardia-Arce, U. Kentsch, A. Eichler-Volf, N. V. Abrosimov, A. Erbe, C. Shin, *et al.*, Metal-assisted chemically etched silicon nanopillars hosting telecom photon emitters, J. Appl. Phys. **132,** 033101 (2022).

[30] M. Khoury, H. Quard, T. Herzig, J. Meijer, S. Pezzagna, S. Cueff, M. Abbarchi, H. S. Nguyen, N. Chauvin, and T. Wood, Light emitting Si-based Mie resonators: Toward a Huygens source of quantum emitters, Adv. Opt. Mat. **10,** 2201295 (2022).

[31] M. Prabhu, C. Errando-Herranz, L. De Santis, I. Christen, C. Chen, and D. R. Englund, Individually addressable artificial atoms in silicon photonics, arXiv:2202.02342.

[32] Y. Baron, A. Durand, T. Herzig, M. Khoury, S. Pezzagna, J. Meijer, I. Robert-Philip, M. Abbarchi, J.-M. Hartmann, S. Reboh, *et al.*, Single G centers in silicon fabricated by co-implantation with carbon and proton, Appl. Phys. Lett. **121,** 084003 (2022).

[33] B. Lefaucher, J.-B. Jager, V. Calvo, A. Durand, Y. Baron, F. Cache, V. Jacques, I. Robert-Philip, G. Cassabois, T. Herzig, *et al.*, Cavity-enhanced zero-phonon emission from an ensemble of G centers in a silicon-on-insulator microring, Appl. Phys. Lett. **122,** 061109 (2023).

[34] L. Komza, P. Samutpraphoot, M. Odeh, Y.-L. Tang, M. Mathew, J. Chang, H. Song, M.-K. Kim, Y. Xiong, G. Hautier, *et al.*, Indistinguishable photons from an artificial atom in silicon photonics, arXiv:2211.09305.

[35] Y. Zhiyenbayev, W. Redjem, V. Ivanov, W. Qarony, C. Papapanos, J. Simoni, W. Liu, K. Jhuria, L. Z. Tan, T. Schenkel, *et al.*, Scalable manufacturing of quantum light emitters in silicon under rapid thermal annealing, Opt. Express **31,** 8352 (2023).

[36] Y. Baron, A. Durand, P. Udvarhelyi, T. Herzig, M. Khoury, S. Pezzagna, J. Meijer, I. Robert-Philip, M. Abbarchi, J.-M. Hartmann, *et al.*, Detection of single W-centers in silicon, ACS Photonics **9,** 2337 (2022).

[37] T. Schenkel, W. Redjem, A. Persaud, W. Liu, P. A. Seidl, A. J. Amsellem, B. Kanté, and Q. Ji, Exploration of defect dynamics and color center qubit synthesis with pulsed ion beams, Quantum Beam Sci. **6,** 13 (2022).

[38] J. Weber, Defect generation during plasma treatment of semiconductors, Physica B **170,** 201 (1991).

[39] I. A. Buyanova, A. Henry, B. Monemar, J. L. Lindström, and G. S. Oehrlein, Photoluminescence of defects induced in silicon by SF_6/O_2 reactive-ion etching, J. Appl. Phys. **78,** 3348 (1995).

[40] G. Andrini, G. Zanelli, S. D. Tchernij, E. Corte, E. N. Hernandez, A. Verna, M. Cocuzza, E. Bernardi, S. Virzí, P. Traina, *et al.*, Efficient activation of telecom emitters in silicon upon ns pulsed laser annealing, arXiv:2304.10132.

[41] K. Murata, Y. Yasutake, K. ichi Nittoh, K. Sakamoto, S. Fukatsu, and K. Miki, Hybrid laser activation of highly concentrated Bi donors in wire-δ-doped silicon, Appl. Phys. Express **3,** 061302 (2010).

[42] R. Monflier, T. Tabata, H. Rizk, J. Roul, K. Huet, F. Mazzamuto, P. Acosta Alba, S. Kerdilès, S. Boninelli, and A. La Magna, *et al.*, Investigation of oxygen penetration during UV nanosecond laser annealing of silicon at high energy densities, Appl. Surf. Sci. **546,** 149071 (2021).

[43] See the Supplemental Material at http://link.aps.org/supplemental/10.1103/PhysRevApplied.0.XXXXXX for details of: (i) a comparison of the effect of the flash annealing on virgin and implanted samples, (ii) a global optical-microscope view of the sample, (iii) the influence of the number of pulses on the ZPLs of G and W centers, (iv) microphotoluminescence spectra and the spatial distribution of the centers in the recrystallized area, and (v) the removal of residual carbon in bulk Si.

[44] J. Bonse, K. W. Brzezinka, and A. J. Meixner, Modifying single-crystalline silicon by femtosecond laser pulses: An analysis by micro Raman spectroscopy, scanning laser microscopy and atomic force microscopy, Appl. Surf. Sci. **221,** 215 (2004).

[45] M. Garcia-Lechuga, N. Casquero, A. Wang, D. Grojo, and J. Siegel, Deep silicon amorphization induced by femtosecond laser pulses up to the mid-infrared, Adv. Opt. Mat. **9,** 2100400 (2021).

[46] C. G. Kirkpatrick, J. R. Noonan, and B. G. Streetman, Recombination luminescence from ion implanted silicon, Radiat. Eff. **30,** 97 (1976).

[47] J. R. Noonan, C. G. Kirkpatrick, and B. G. Streetman, Low-temperature photoluminescence from boron ion implanted Si, Radiat. Eff. **21,** 225 (1974).

[48] V. D. Tkachev, C. Schrödel, and A. V. Mudryi, Annealing of lattice damage in ion implanted silicon, Radiat. Eff. **49,** 133 (1980).

[49] H. Feick and E. R. Weber, Annealing of the photoluminescence W-center in proton-irradiated silicon, Phys. B: Condens. Matter **273-274,** 497 (1999).

[50] G. Davies and K. T. Kun, Annealing the di-carbon radiation damage centre in silicon, Semicond. Sci. Technol. **4,** 327 (1989).

[51] R. Pässler, Basic model relations for temperature dependencies of fundamental energy gaps in semiconductors, Phys. Stat. Sol. (b) **200,** 155 (1997).

[52] M. Cardona and M. L. W. Thewalt, Isotope effects on the optical spectra of semiconductors, Rev. Mod. Phys. **77,** 1173 (2005).

[53] S. Rudin, T. L. Reinecke, and B. Segall, Temperature-dependent exciton linewidths in semiconductors, Phys. Rev. B **42,** 11218 (1990).

[54] P. Borri, W. Langbein, U. Woggon, M. Schwab, M. Bayer, S. Fafard, Z. Wasilewski, and P. Hawrylak, Exciton dephasing in quantum dot molecules, Phys. Rev. Lett. **91,** 267401 (2003).

[55] Y.-C. Chen, P. S. Salter, M. Niethammer, M. Widmann, F. Kaiser, R. Nagy, N. Morioka, C. Babin, J. Erlekampf, P. Berwian, *et al.*, Laser writing of scalable single color centers in silicon carbide, Nano Lett. **19,** 2377 (2019).

[56] Y.-C. Chen, B. Griffiths, L. Weng, S. S. Nicley, S. N. Ishmael, Y. Lekhai, S. Johnson, C. J. Stephen, B. L. Green, G. W. Morley, *et al.*, Laser writing of individual nitrogen-vacancy defects in diamond with near-unity yield, Optica **6,** 662 (2019).

[57] K. Jhuria, V. Ivanov, D. Polley, W. Liu, A. Persaud, Y. Zhiyenbayev, W. Redjem, W. Qarony, P. Parajuli, Q. Ji, *et al.*, Programmable quantum emitter formation in silicon, arXiv:2307.05759.